Electronic Supplementary Material (ESI) for Journal of Materials Chemistry C.

Influence of codoped Gd^{3+} ions on spectroscopic site symmetry of Dy^{3+} ions in LaF_3 single crystal

Mingyuan Hu,[ab] Yan Wang,[a] Zhenyu You,[a] Zhaojie Zhu,[a] Jianfu Li,[a] Xiuyuan Cai,[ab] and Chaoyang Tu*[a]

[a]Key Laboratory of Optoelectronic Materials Chemistry and Physics, Fujian Institute of Research on the Structure of Matter, Chinese Academy of Sciences, Fuzhou City, Fujian Province 350002, P. R. China
[b]University of Chinese Academy of Science, Beijing, 100039, P. R. China

Theoretical studies

The structural optimization of pure and doped LaF_3 crystal was performed by the BFGS geometry optimization method in the total-energy code castep of materials studio.[1, 2] The schematic representation of LaF_3 crystals are shown in Figure S1. The initial structure of pure LaF_3 was output from ICSD database (No. 3) as shown in Figure S1a.[3] First, the cell parameters of pure LaF_3 were obtained in table S1,[4] and the final LaF9 polyhedron is shown in Figure S1d. Then, the starting structures of Dy^{3+} and Gd^{3+} doped LaF_3 were built with the $1 \times 1 \times 2$ supercell of optimized LaF_3 structure, and one La was substituted by Dy and Gd, respectively (Figure S1b and S1c). The quality of geometry optimization was set as customized performed with the energy of 2.0×10^{-5} eV/atom, a convergence threshold of 0.05 eV/Å on the max force, 0.01 GPa on the max stress, and 0.002 Å on the max displacement. The electronic structures including band structure and density of state (DOS) calculations were performed by using a plane-wave basis set and pseudopotentials. The following valence electron configurations were considered in the computation: F-$2s^2 2p^5$, La-$5s^2 5p^6 5d^1 6s^2$, Gd-$4f^7 5s^2 5p^6 5d^1 6s^2$, and Dy-$4f^{10} 5s^2 5p^6 6s^2$. The exchange and correlation effects were treated by Perdew-Burke-Ernzerhof (PBE) in the generalized gradient approximation (GGA).[5] The interactions between the ionic cores and the valence elections were described by the ultrasoft pseudopotential.[6] The number of plane waves included in the basis sets was determined by the cutoff energy of 550 eV, and the numerical integration of the Brillouin zone was performed by using Monkhorst-Pack k-point sampling of $2 \times 2 \times 1$. The final DyF9 and GdF9 polyhedrons are shown in Figure S1e and S1f, and the calculated electronic structures are in Figure 3S.

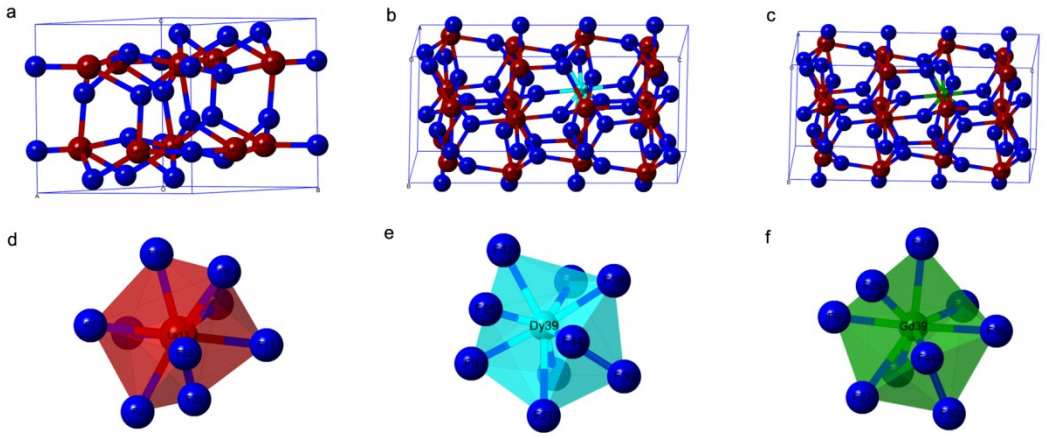

Figure S1. The initial crystal structure model for geometry optimization (a: LaF_3, b: Dy:LaF_3, c: Gd:LaF_3), and the final LaF9(d), DyF9(e) and GdF9(f) polyhedrons.

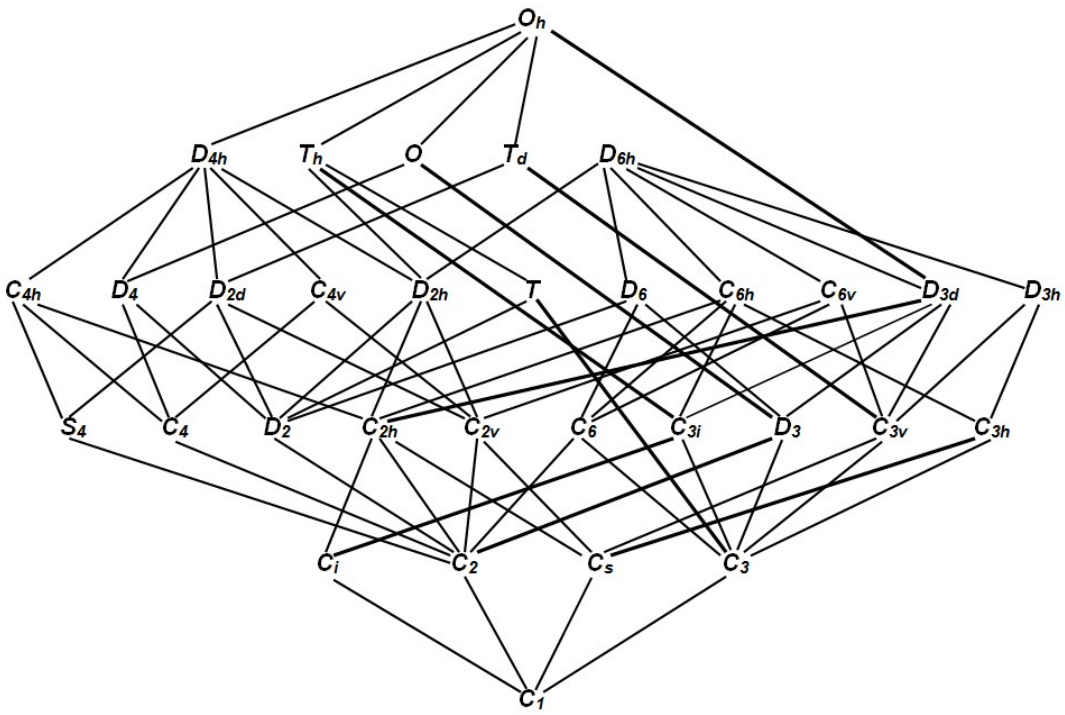

Figures S2. Branching rules of the 32 crystallographic point groups.[7]

Table S1. Positional parameters and site occupation factors (SOF) of optimized trigonal LaF_3 crystals.

Phase	Atom	Site	x/a	y/b	z/c	SOF
Trigonal ($P\bar{3}C1$) a=b=7.322Å c=7.501Å	La	6f	0.65728	0	0.25	1
	F1	12g	0.37009	0.05951	0.08102	1
	F2	4d	0.33333	0.66667	0.18509	1
	F3	2a	0	0	0.25	1

Table S2. The bong length of La-F, Dy-F and Gd-F, which show the structural information of LaF9, DyF9 and GdF9 polyhedrons as shown in figure S1d, S1e and S1f.

Bond	Bond length (Å)	Bond	Bond length (Å)	Bond	Bond length (Å)
La13-F1	2.671	Dy39-F9	2.336	Gd39-F9	2.363
La13-F2	2.522	Dy39-F25	2.468	Gd39-F25	2.406
La13-F5	2.671	Dy39-F27	2.612	Gd39-F27	2.596
La13-F6	2.522	Dy39-F28	2.529	Gd39-F28	2.493
La13-F7	2.512	Dy39-F30	2.668	Gd39-F30	2.727
La13-F11	2.512	Dy39-F36	2.361	Gd39-F36	2.436
La13-F19	2.456	Dy39-F43	2.327	Gd39-F43	2.372
La13-F20	2.456	Dy39-F44	2.334	Gd39-F44	2.376
La13-F23	2.509	Dy39-F47	2.430	Gd39-F47	2.406

Table S3. The Interionic distance of La13-La, Dy39-La and Gd39-La.

	Interionic distance (Å)		Interionic distance (Å)		Interionic distance (Å)
La13-La14	4.169	Dy39-La16	4.472	Gd39-La16	4.512
La13-La14	4.169	Dy39-La17	4.477	Gd39-La17	4.456
La13-La14	4.346	Dy39-La18	4.362	Gd 39-La18	4.374
La13-La15	4.169	Dy39-La37	4.517	Gd 39-La37	4.355
La13-La15	4.169	Dy39-La37	4.517	Gd 39-La37	4.133
La13-La15	4.346	Dy39-La37	4.376	Gd 39-La37	4.200
La13-La16	4.401	Dy39-La38	4.371	Gd 39-La38	4.354
La13-La16	4.401	Dy39-La38	4.171	Gd 39-La38	4.136
La13-La17	4.513	Dy39-La38	4.145	Gd 39-La38	4.196
La13-La17	4.513	Dy39-La40	4.377	Gd 39-La40	4.517
La13-La18	4.513	Dy39-La41	4.126	Gd 39-La41	4.510
La13-La18	4.513	Dy39-La42	4.185	Gd 39-La42	4.403

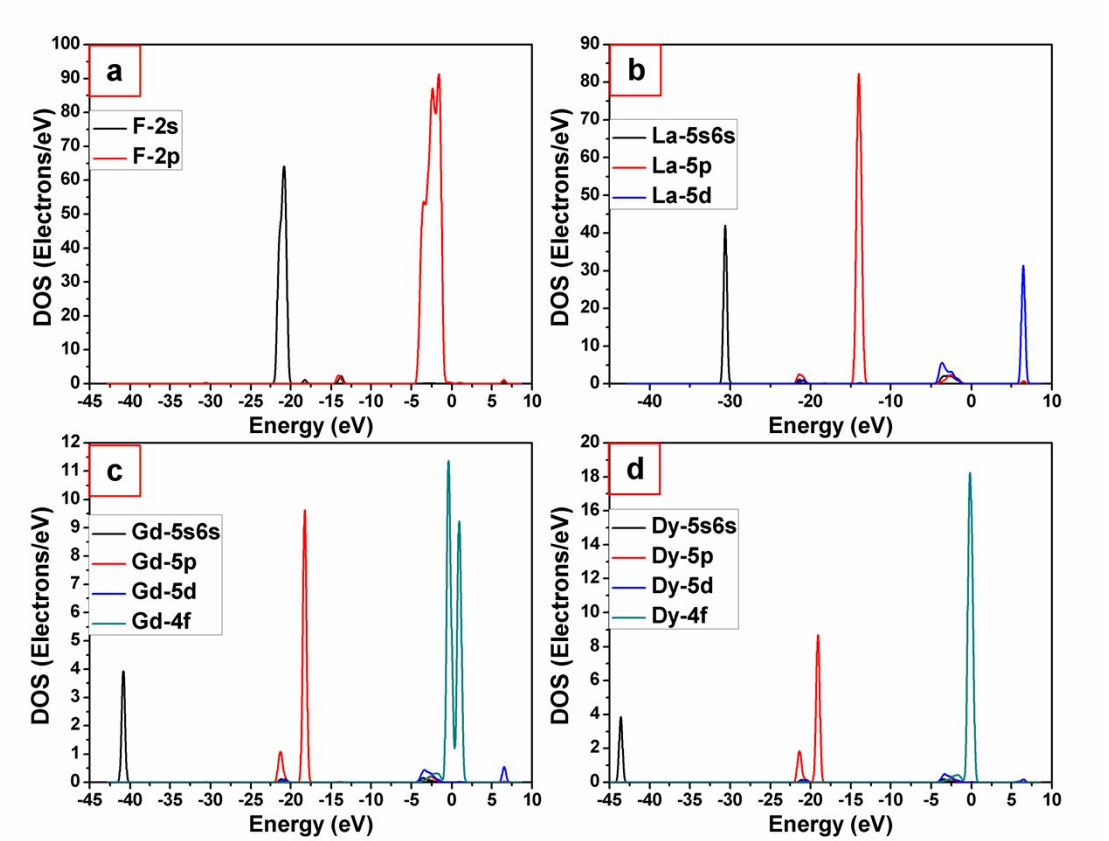

Figure S3. Calculated electronic DOS of the supercell of Dy/Gd:LaF_3, (a) the partial DOS of F, (d) the partial DOS of La, (e) the partial DOS of Gd, (f) the partial DOS of Dy.

Table S4. The energy level of $^6H_{15/2}$, $^6H_{13/2}$, $^4F_{7/2}$, and $^4I_{15/2}$ of Dy^{3+} in LaF_3 at 77 K (Exp. = Experimental).

SLJ State	Energy (cm^{-1})		SLJ State	Energy (cm^{-1})	
	Exp.	Fit[8]		Exp.[a]	Fit[8]
$^6H_{15/2}$		0	$^4F_{9/2}$	21053	21058
		28		21108	21131
		76		21164	21147
		126		21220	21190
		188		21413	21358
		209	$^4I_{15/2}$	21978	22022
		296		22039	22132
		316		22087	22175
$^6H_{13/2}$		3502		22148	22189
		3568		22222	22213
		3602		22297	22292
		3624		22346	22342
		3639		22384	22379
		3678			
		3681			

[a]The experimental data were obtained from the excitation spectra.

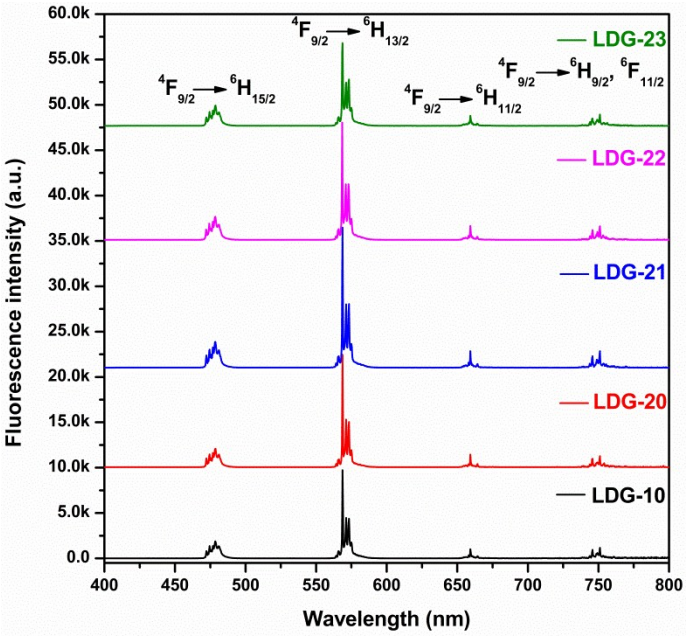

Figure S4. Visible emission spectra of Dy^{3+}/Gd^{3+} codoped LaF_3 single crystals pumped by 349 nm at 77 K.

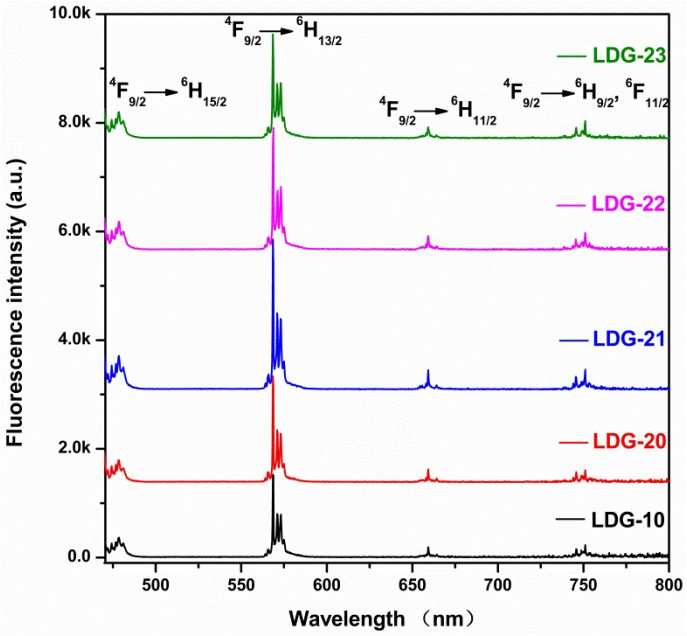

Figure S5. Visible emission spectra of Dy^{3+}/Gd^{3+} codoped LaF_3 single crystals pumped by 453.75 nm at 77 K.

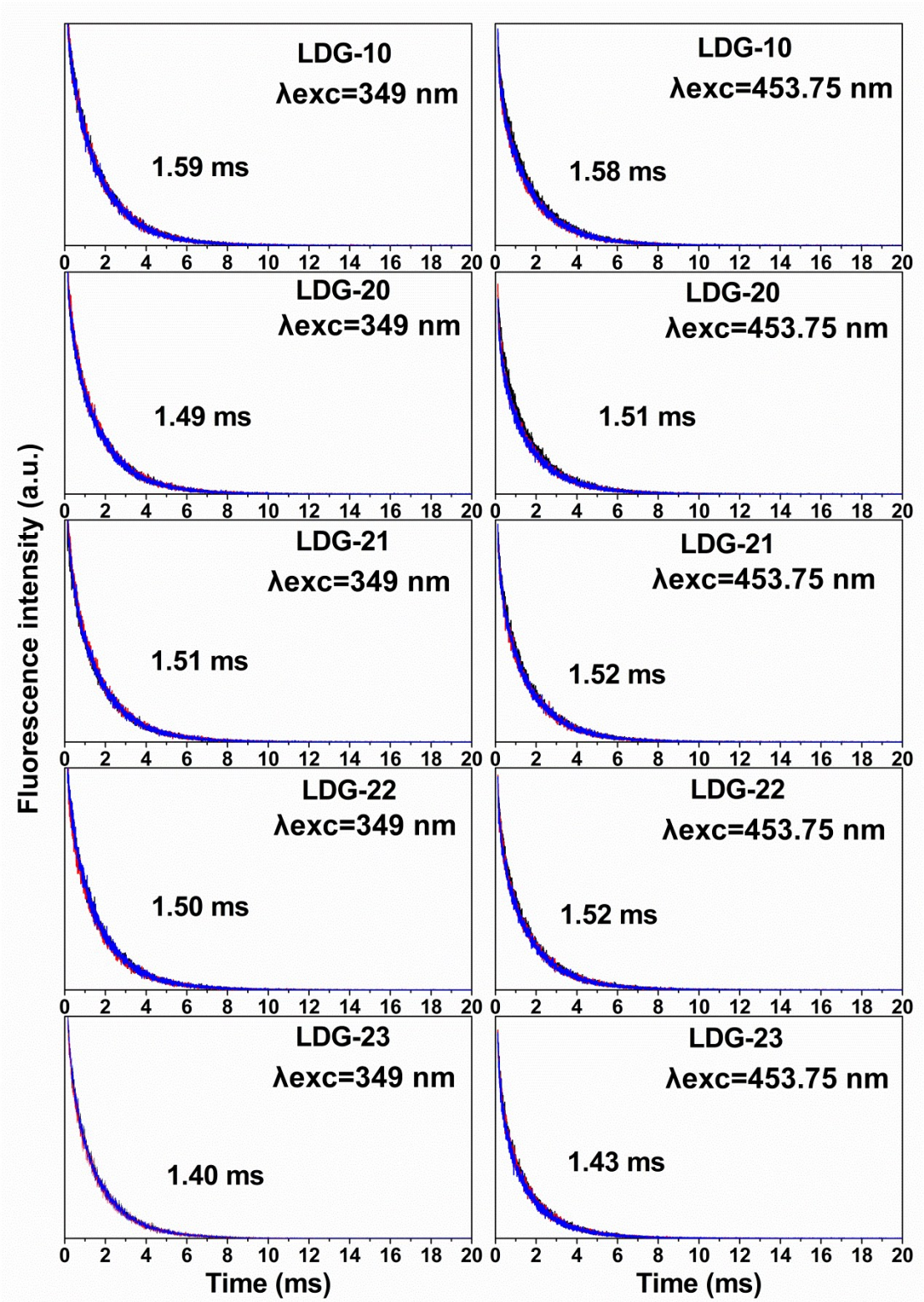

Figure S6. The yellow fluorescence decay curves of 568.75 nm, 571.25 nm, and 573.25 nm with the excitation of 349 nm and 453.75 nm in LDG crystals at 77 K.

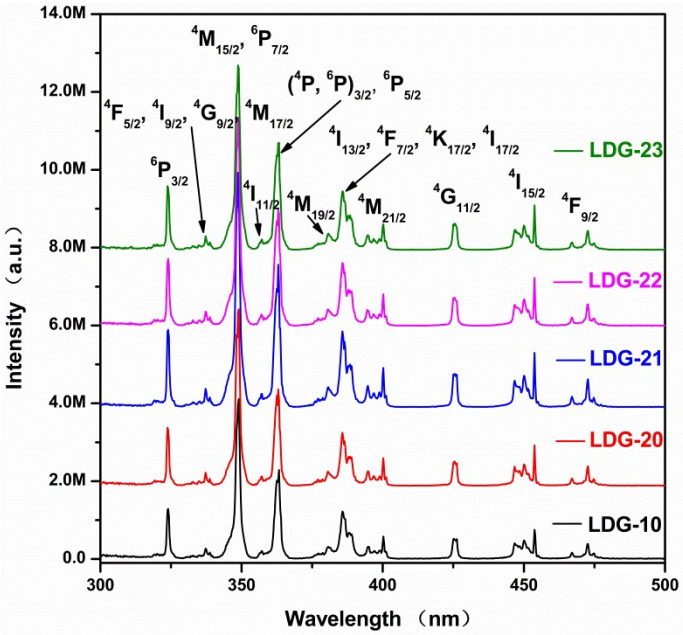

Figure S7. 77 K PL excitation (λ_{em}=568.75 nm) spectra of Dy^{3+}/Gd^{3+} codoped LaF_3 single crystals.

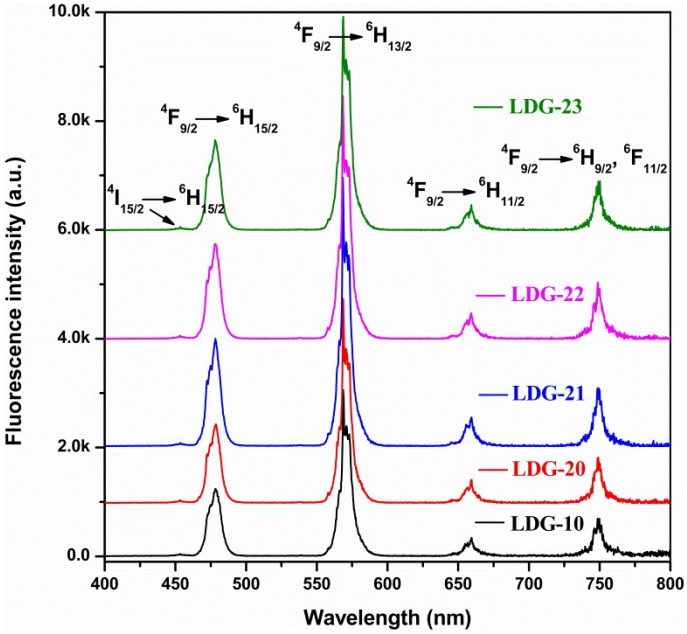

Figure S8. Visible emission spectra of Dy^{3+}/Gd^{3+} codoped LaF_3 single crystals pumped by 349 nm at 298 K.

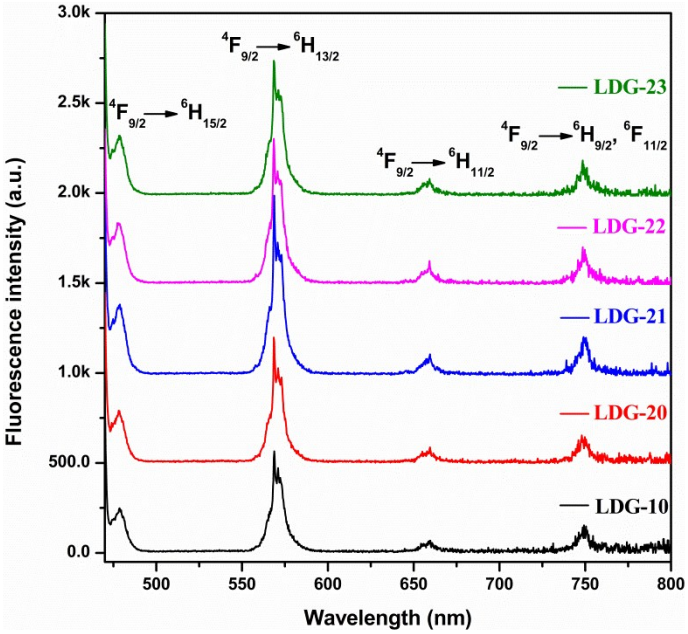

Figure S9. Visible emission spectra of Dy^{3+}/Gd^{3+} codoped LaF_3 single crystals pumped by 453.75 nm at 298 K.

CIE Chromaticity Coordinates

The assessment and quantification of color is referred to as colorimetry or the 'science of color'. The CIE 1931 diagram is the universally accepted system to represent the composition of any color by means of three primary colors. To describe the color produced by any light source, three color matching functions such as $\bar{x}(\lambda)$, $\bar{y}(\lambda)$, and $\bar{z}(\lambda)$ are essential. Artificial "colors", denoted by X, Y and Z, also called tristimulus values, can be added to produce real spectral colors. The degree of simulation required to match the color of given power spectral density ($P(\lambda)$) can be expressed as[9]

$$X = \int \bar{x}(\lambda)P(\lambda)d\lambda \quad (1)$$

$$Y = \int \bar{y}(\lambda)P(\lambda)d\lambda \quad (2)$$

$$Z = \int \bar{z}(\lambda)P(\lambda)d\lambda \quad (3)$$

where X, Y and Z are the tristimulus values which give the simulation for each three primary colors required to match the color of the given ($P(\lambda)$). By using these tristimulus values, the chromaticity coordinates (x,y) of the studied LDG crystals can be evaluated from the following expressions,

$$x = \frac{X}{X+Y+Z} \quad (4)$$

$$y = \frac{Y}{X+Y+Z} \quad (5)$$

The calculated chromaticity coordinate (x,y) values are shown in Figure S10.

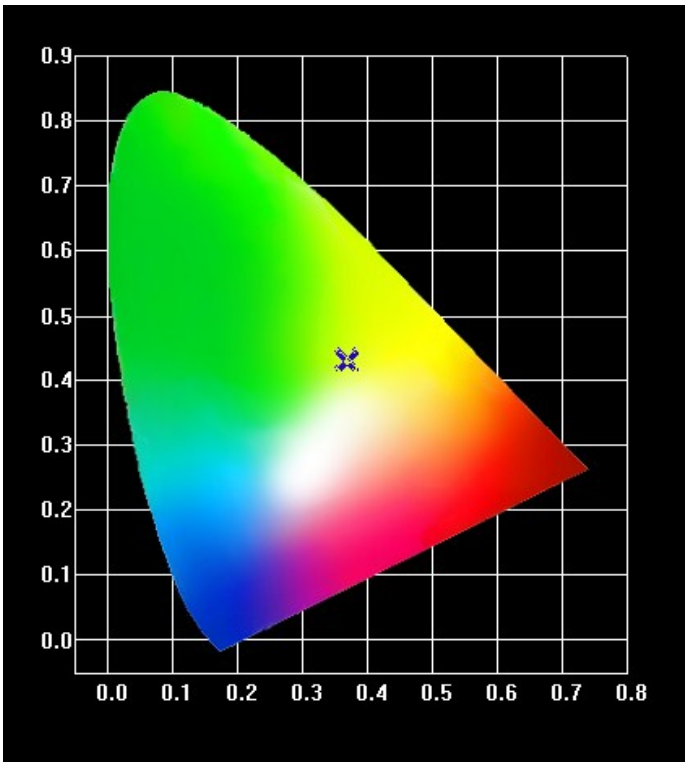

Figure S10. CIE-1931 chromaticity diagram of LDG crystals under 349 nm and 453.75 nm excitation at 298 K.

Energy transfer mechanism

The critical transfer distance between Dy^{3+} ions (R_c) for energy transfer was calculated using the critical concentration of the activator ions[10]

$$R_c \approx 2\left(\frac{3V}{4\pi x_c Z}\right)^{\frac{1}{3}} \quad (6)$$

where V represents the volume of the unit cell, x_c stands for the critical concentration of the activator ion and Z refers to the number of formula units per unit cell. For LaF_3 crystal, V=328.65 $Å^3$, and Z=6. The x_c are 0.01 and 0.02 in LDG-10 and LDG-20 respectively. The R_c are calculated to be about 21.87 Å and 17.36 Å in LDG-10 and LDG-20 respectively.

Based on Van Uitert's model,[11] the energy transfer mechanism between the activator ions can be confirmed by investigating the emission intensity (I) per activator ion concentration (x) in terms of the following equation

$$\frac{I}{x} = \frac{k}{I + \beta(x)^{\frac{\theta}{3}}} \quad (7)$$

where k and β are constants for the same excitation condition for the given host, and x is the activator concentration which is not less than the critical concentration. The above equation (7) can be rearranged for $\beta(x)^{\theta/3} \gg 1$ as follows[12]

$$\lg\left(\frac{I}{x}\right) = K' - \frac{\theta}{3}\lg(x) \quad (8)$$

Where $K' = \lg k - \lg\beta$ is a constant, θ is the constant of multipolar interaction and is equal to 3,6,8,10 for the nearest neighbour ions (θ=3), dipole-dipole (θ=6), dipole-quadrupole (θ= 8) and quadrupole-quadrupole (θ=10) interactions respectively. Using the yellow fluorescence emissions of LDG-10 and LDG-20 shown in Figure S8 and S9, the θ was determined to be 2.1. So the the nearest neighbour ions play a major role for concentration quenching in Dy^{3+} doped LaF_3 crystals.

References

[1] B. G. Pfrommer, M. Cote, S. G. Louie and M. L. Cohen, *J. Comput. Phys.*, 1997, 131, 233-240.

[2] S. J. Clark, M. D. Segall, C. J. Pickard, P. J. Hasnip, M. J. Probert, K. Refson and M. C. Payne, *Zeitschrift für Kristallographie-Crystalline Materials*, 2005, 220, 567-570.

[3] A. K. Cheetham, B. E. F. Fender, H. Fuess and A. F. Wright, *Acta Crystallogra. B*, 1976, 32, 94-97.

[4] M. Hu, Z. Zhu, Y. Wang, J. Li, Z. You and C. Tu, *Cryst. Growth Des.*, 2018, 18, 5981-5990.

[5] J. P. Perdew, K. Burke, M. Ernzerhof, *Phys. Rev. Lett.*, 1996, 77, 3865-3868.

[6] N. Troullier, J. L. Martins, *Phys. Rev. B*, 1991, 43, 1993-2006.
[7] P. H. Butler, *Point Group Symmetry Application: Method and Tables*, Plenum, New York, 1981.
[8] W. T. Carnall, G. L. Goodman, K. Rajnak, R. S. Rana, *J. Chem. Phys.*, 1989, 90, 3443-3457.
[9] P. Suthanthirakumar and K. Marimuthu, *J. Mol. Struct.*, 2016, 1125, 443-452.
[10] Z. Xiu, S. Liu, M. Ren, J. Liu, J. Pan and X. Cui, *J. Alloy. Compd.*, 2006, 425, 261-263.
[11] D. L. Dexter, *J. Chem. Phys.*, 1953, 21, 836-850.
[12] M. Jayachandiran and S. M. M. Kennedy, *J. Alloy. Compd.*, 2019, 775, 353-359.